npj | clean water

www.nature.com/npjcleanwater

ARTICLE OPEN

Check for updates

Effective pathogen removal in sustainable natural fiber Moringa filters

Laxmicharan Samineni[1], Sophie De Respino[2], Yu-Ming Tu[1], Ratul Chowdhury[3], Rashmi Prava Mohanty[4], Hyeonji Oh[1], Michael Geitner[3], Claire Hartwig Alberg[5], Abigail Roman-White[3], Sarine McKinzie[3], Camila Lemus[3], Joy Massey[6], Debadyuti Ghosh[4], Thomas M. Truskett[1], Stephanie Velegol[3] and Manish Kumar[1,2]✉

Pathogen contamination of water has a massive impact on global human health. In particular, viruses pose unique challenges to water treatment techniques due to their small size and presence in water as both individual virions and when absorbed onto larger particles. Low-energy water treatment processes such as media filtration are not capable of completely removing viruses owing to their small size. Hence, less sustainable processes with high chemical or energy consumption such as chemical disinfection, ultraviolet irradiation, and membrane filtration are usually required. To overcome high energy and/or chemical requirements for virus treatment, designs for sustainable fiber filters fabricated from minimally processed natural materials for efficient virus (MS2) and bacteria (*E. coli*) removal are presented in this work. These filters were created by functionalizing readily accessible natural fibers including cotton, silk, and flax with a simple aqueous extract containing cationic proteins from *Moringa oleifera* seeds. The proposed filters offer a comprehensive low cost, low energy, and low environmental impact solution for pathogen removal from water with removals of >7log$_{10}$ (99.99999%) for viruses and bacteria.

npj Clean Water (2022)5:27 ; https://doi.org/10.1038/s41545-022-00170-5

INTRODUCTION

Drinking water treatment plants can act as critical reservoirs for the accumulation and release of harmful biological and chemical contaminants because they exist at the interface of nature and human habitats[1]. Thus, developing water treatment techniques to remove contaminants from water has been a fundamental engineering endeavor. Human enteric viruses are an important contaminant in water that can cause devastating impacts on global human health[2]. Media filtration is a basal unit operation in water treatment that has low energy intensity and is globally implementable. However, it only offers partial virus removal even when combined with chemical coagulation[3]. Hence, energy-intensive UV disinfection or chemical-intensive chlorine disinfection is widely used in conjunction with filtration to achieve regulated drinking water treatment standards. For example, the US Environmental Protection Agency (EPA) and World Health Organization (WHO) both require a 4 log$_{10}$ (99.99%) virus removal and/or inactivation for drinking water[4]. Another alternative proposed for achieving effective virus removal is energy-intensive and expensive modes of filtration based on nano-porous membranes such as ultrafiltration or nanofiltration[5,6].

Efforts to develop effective water treatment technologies for virus removal represent a striking example of the trade-off between clean water quality and associated energy consumption for production[7] (Fig. 1). First, the reliance on size-exclusion based membranes to replace ineffective conventional filtration gives rise to a trade-off between the productivity and the removal efficiency achieved (Fig. 1a). Second, chlorination widely used as an alternative or in conjunction with conventional filtration leads to the formation of disinfection byproducts (DBPs) that have been linked to cancer and other health effects[8]. Alternative disinfection technologies under consideration to mitigate these adverse health effects such as ozone and UV irradiation are, again, expensive and energy-intensive[9]. When the embedded energy for processing the materials and chemicals required is compared among available techniques, the total energy requirement of most disinfection technologies (except chlorination) is on par with energy-intensive membrane filtration (Fig. 1b). Recent studies propose chemical functionalization of low-pressure membranes or specialized membrane fabrication techniques such as electrospinning and the use of nanofibrous materials to improve the energy-efficiency of membrane filtration[10–13]. However, the need for advanced fabrication/modification strategies impedes their widespread use. Therefore, to overcome the challenges with virus treatment, it is crucial to develop novel filtration techniques that can overcome the productivity and efficiency trade-off (Fig. 1a) using materials with low embedded energy. Minimally processed natural materials with low carbon footprint and low environmental impact such as those utilized in this work could provide a solution to this trade-off.

Overall, there is an emerging need for the control of pathogen contamination, especially viruses, from water systems using sustainable approaches. In this work, the feasibility of using a sustainable depth filter fabricated from easily accessible materials that can be deployed with minimal cost to achieve highly efficient removal of pathogens from water was demonstrated (Fig. 2a). These filters were designed by leveraging the water clarification function[14] and antimicrobial[15] activity of *Moringa oleifera* (*MO*) seeds. The *MO* tree is prevalent throughout tropic and sub-tropic regions, and its seeds have been historically used as a natural

[1]McKetta Department of Chemical Engineering, University of Texas at Austin, Austin, TX 78712, USA. [2]Department of Civil, Architectural and Environmental Engineering, University of Texas at Austin, Austin, TX 78712, USA. [3]Department of Chemical Engineering, The Pennsylvania State University, University Park, Pennsylvania, PN 16802, USA. [4]Division of Molecular Pharmaceutics and Drug Delivery, College of Pharmacy, The University of Texas at Austin, Austin, TX 78712, USA. [5]Department of Civil, Environmental and Geo-Engineering, College of Science and Engineering, University of Minnesota, Minneapolis, MN 55455, USA. [6]Department of Chemical Engineering, Tuskegee University, Tuskegee, AL 36088, USA. ✉email: manish.kumar@utexas.edu

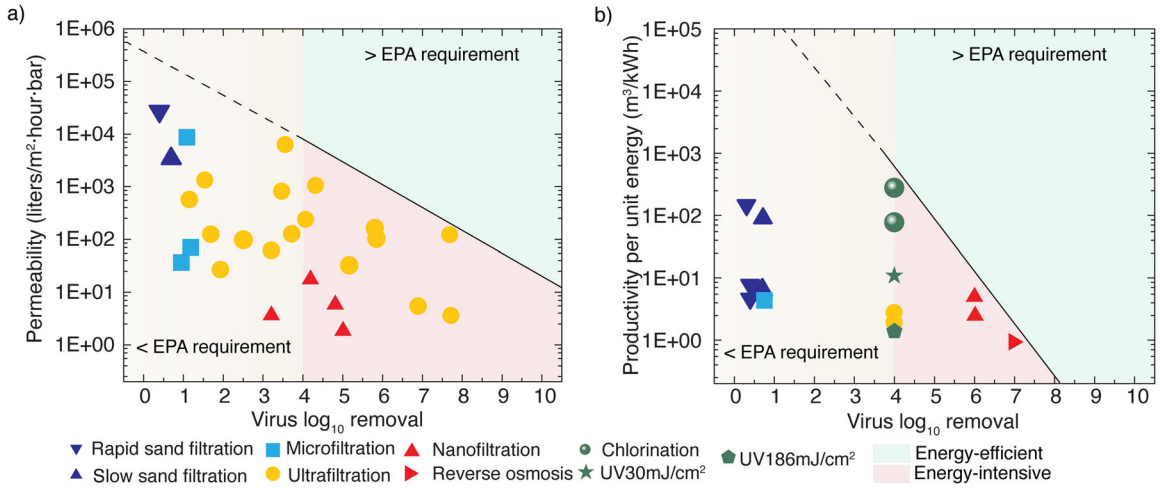

Fig. 1 A pathogen removal vs. productivity trade-off exists in virus filtration techniques widely used in water treatment illustrating the challenge with virus removal. a The permeability vs. virus retention efficiency of widely used filtration technologies shows that a trade-off exists between the pathogen removal and permeability due to the dependence on size-exclusion. The tabulated data with references is available in Supplementary Table 4. **b** The operational energy requirement of filtration techniques and total energy requirement of disinfection techniques (except for chlorination) considering a combination of operational energy and embedded chemical energy is comparable. This indicates that filtration techniques can potentially achieve similar performance as disinfection, specifically if the virus removal efficiency can be increased without incurring substantial additional operational energy costs. A detailed summary of the literature survey and energy requirement values used can be found in Supplementary Table 5 and Supplementary Note 2.

coagulant[14,16]. Aqueous extracts from *MO* seeds contain two cationic proteins, *MO* coagulant protein (MO2.1) and *MO* chitin binding protein (MoCBP), with established antifungal and coagulant activities[14,17,18]. *MO* seeds are an ideal candidate for application in water treatment due to the prolific nature of the *MO* tree (15,000–20,000 seeds per tree per year)[19] and the low toxicity of aqueous seed extract[20]. We developed and tested the capability of *MO* protein functionalized natural fiber filters to remove both viruses and bacteria from water at unprecedented levels. This proposed platform technology shows potential for application at community or point-of-use scales in a wide range of public health scenarios including disaster preparedness.

RESULTS

Easily accessible natural fibers can be used to build microporous filters and effectively functionalized with simple water extract from *MO* seeds

The main findings of this study are that a simple water extract from *MO* seeds can be used to successfully functionalize accessible substrates with cationic proteins, which can then be used as an affinity-based filter to remove contaminants from water. In our previous work, it was shown that model sand particles can be functionalized by this proposed process to achieve high pathogen removal[21,22]. However, challenges related to the effect of flowrate (low filter loading rate in the range of slow sand filtration) and functional sand grain size (<130 µm, which is difficult to source) restrict the applicability of the functionalized sand filters under practical conditions. In this study, inspired by fibrous filter media used extensively for air filtration[23], commonly available low-cost natural fibers were used as potential substrates for fabricating *MO*-functionalized depth filters. Note that the use of minimally processed natural fibers as substrates in depth filters for water treatment has not been explored before. Three natural fiber sources—unprocessed cotton balls, flax fiber, and silk fiber, from local and online stores accessible worldwide (see Supplementary Methods for details) were used in this study. A thorough chemical and morphological characterization of individual fibers was first performed. Fourier-transform infrared spectroscopy (FTIR) and Scanning electron microscopy (SEM) analyses shown in Fig. 2b, c indicated that the fibers procured from local sources exhibit similar characteristics as standard fiber samples[24].

Next, the depth filters built by packing the three natural fibers were characterized using Brunauer–Emmett–Teller (BET) analysis, capillary flow porometry, electrokinetic analysis, and a fluorometric peptide (protein quantification) assay to measure the specific surface area, pore size, surface charge, and protein adsorbed per unit surface area of the fiber. Maintaining a constant height of packing and weight of fiber used per filter across the board was difficult due to inherent differences in the fiber properties, so the final properties shown below were normalized to unit volume and surface area. The weight of the fiber, the height of packing, and packing density used for cotton, silk, and flax fibers in this study are detailed in Supplementary Table 3. The results from BET analysis and capillary flow porometry showed that cotton, silk, and flax can form micro-porous depth filters with high surface area (Fig. 3a, b). The mean pore sizes of cotton, silk, and flax fiber filters were 6.54 ± 1.64 µm, 7.48 ± 0.78 µm, and 11.1 ± 4.51 µm, respectively. These results show that the fiber filters proposed in this study show low mean pore size and high specific surface area compared to sand filters from previous work[21]. These favorable characteristics enable *MO*-functionalized fiber filters to effectively capture viruses at higher flowrates compared to sand filters (Fig. 6a, b).

The surface charge of the fibers packed in a depth filter is critical to enabling the adsorption of *MO* proteins during functionalization. The results from the electrokinetic analysis showed (Fig. 3c) that all three fibers tested in this study are negatively charged in the pH range of 5–8 (−2.4 mV to −20.2 mV), which is favorable for the adsorption of cationic proteins. Note that the average streaming potential of the natural fibers at a pH of 7 was shown in Fig. 3c to represent the neutral pH conditions. Please refer to Supplementary Fig. 2 for the streaming potential results from the analysis conducted at additional pH conditions of 5, 6, and 8. To establish the feasibility of functionalizing the proposed fiber filters with *MO* seed proteins, experiments were conducted by flowing a simple water extract of *MO* seed powder through the filters. The water extract was made by mixing ground *MO* seed with water (0.02 g mL^{-1} w v^{-1} of seed to water) for 5 min before filtering the seed debris out. This analysis showed that

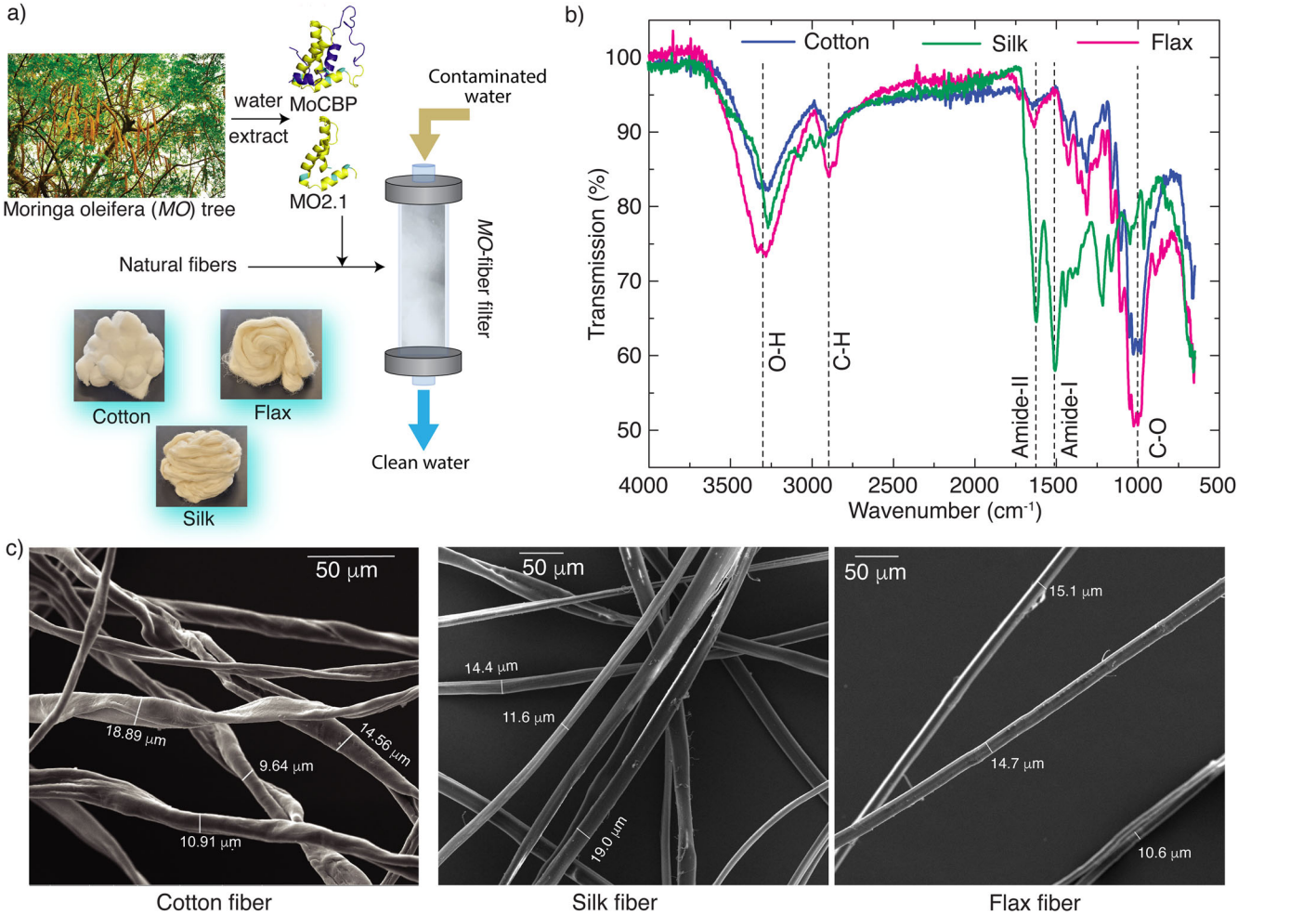

Fig. 2 Easily accessible natural fibers offer an efficient substrate for functionalization with *Moringa oleifera* seed proteins. a A simple schematic of the proposed natural fiber filters functionalized with *MO* proteins in this study. The picture of Moringa tree by Prof. Chen Hualin is licensed under CC BY-SA 4.0 **b** Fourier-transform infrared spectroscopy analysis of cotton, silk, and flax fibers show the presence of C-H, O-H, C-O peaks in cotton and flax representative of cellulose[50]. Silk fibers show the presence of Amide-I (C=O bond stretching) and Amide-II (N-H bending and C-N stretching) peaks indicative of silk fibroin[51]. **c** Scanning electron microscopy images of cotton, silk, and flax fibers show typical fiber diameters (10–20 μm) and morphologies of the natural fibers.

protein adsorbed on the fiber filters was between 6.28 ± 0.42 mg m^{-2} and 11.36 ± 1.72 mg m^{-2} (Fig. 3d). A qualitative comparison of the adsorbed proteins using SDS-PAGE gel electrophoresis also showed no significant change in the protein composition (Supplementary Fig. 3). Overall, it was demonstrated for the first time that a range of easily available natural fibers can be used to build negatively charged microporous depth filters that can be effectively functionalized with a simple water extract from *MO* seeds.

MO functionalization of natural fiber filters enhances their pathogen removal efficiency by ~7 orders of magnitude

A series of standard filtration experiments were performed to quantify the effectiveness of functionalizing the fiber filters with *MO* seed proteins for pathogen capture and removal. The experiments were performed with model organisms for bacteria (*E. coli*) and surrogate viruses (MS2 bacteriophage). *E. coli* is an important model bacteria in the context of water purification that can cause diarrhea and gastrointestinal complications by itself[25]. The removal of MS2 bacteriophage was explored due to its wide use as a surrogate for human enteric viruses such as norovirus and rotavirus[26]. These experiments demonstrated that *MO*-functionalized fiber filters achieve pathogen removal efficiencies that are multiple orders of magnitude higher than the uncoated fiber filters at the same flowrate. For example, at a flowrate of 2 mL min^{-1}, *MO*-cotton filters achieved a log removal efficiency (LRE) of >7.62 for *E. coli* and 7.65 ± 0.23 for MS2 bacteriophage compared to 0.39 ± 0.51 for *E. coli* and 0.23 ± 0.20 for MS2 achieved by uncoated cotton filters (Fig. 4a, c). *MO*-functionalized flax and silk filters also achieved bacteria and virus removal efficiencies similar to *MO*-cotton filters. The LRE achieved in this study is similar to that achieved by *MO*-sand filters reported in previous studies[21]. The advantage of the *MO*-functionalized fiber filters proposed in this study is that they retain this high removal efficiency at flowrates approximately four times higher than *MO*-sand filters (Fig. 6a, b). This shows that natural fibers offer an effective substrate for *MO* protein functionalization compared to sand.

Traditional filtration theory can be used to gain a perspective of the advantage, in terms of removal, due to the *MO*-functionalization of natural fiber filters. According to standard clean-bed filtration theory, the removal of particles in a depth filter mainly depends on two factors: the collision efficiency and the sticking coefficient[27]. The collision efficiency represents the transport of particles to the surface of a collector (substrate) that results in the collisions required for their capture. This depends

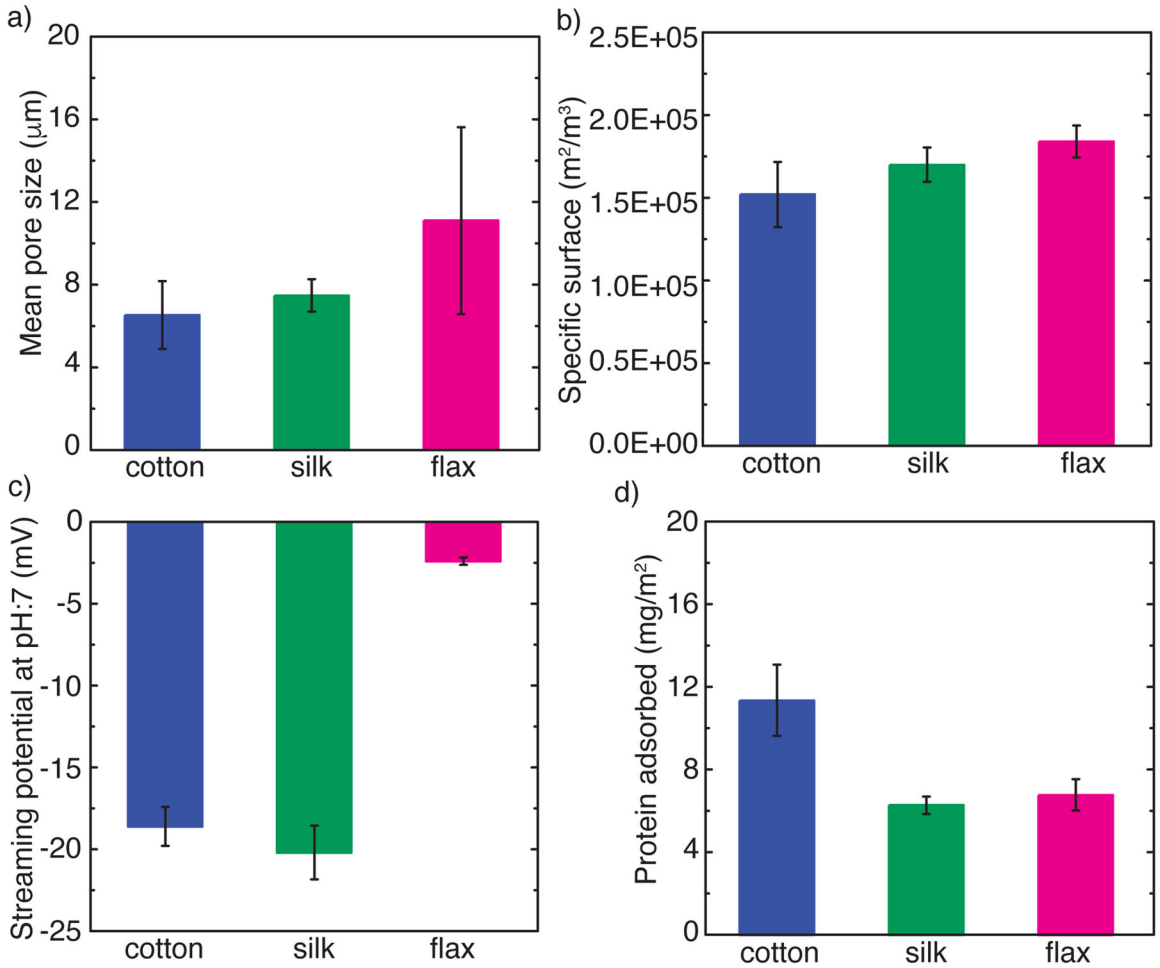

Fig. 3 Standard characterization shows that cotton, flax, and silk fibers can be packed into microporous depth filters that can be easily functionalized with *MO* water extract. a The mean pore size of fiber filters was measured using a capillary flow porometer with water as a wetting liquid. The results show that cotton, silk, and flax fiber filters exhibit a mean pore size of 6.54 ± 1.64 μm, 7.48 ± 0.78 μm, and 11.1 ± 4.51 μm, respectively. **b** The specific surface area estimated using BET adsorption analysis showed that cotton, silk, and flax filters offer similar high surface filters for *MO* functionalization. **c** The streaming potential measurements of uncoated natural fibers indicate that they are negatively charged (−2.4 ± 0.23 mV to −20.2 ± 1.64 mV at pH: 7) favoring the adsorption of *MO* cationic proteins. The streaming potential measurements in the pH range of 5 to 8 are shown in Supplementary Fig. 2. **d** Quantification of *MO* protein adsorbed on the surface of natural fiber filters desorbed using 600 mM NaCl solution shows that cotton has the highest protein adsorption capacity. All the error bars shown in the figure represent the standard deviation calculated from three independent measurements.

primarily on the geometry of the filter, substrate size, and the hydrodynamics of the filter. The transport mechanism for the collisions could be a combination of diffusion, interception, and sedimentation depending on the particle size[27]. When a particle collides with the substrate, it will be captured if the particle successfully attaches to the substrate. A sticking coefficient is traditionally used to define the efficiency of attachment, and it depends on the buffer and substrate chemistry[28]. Therefore, two filters with similar geometries, substrate size, and hydrodynamics can achieve significantly different removals depending on how the substrate interacts with the particles. To show that the high efficiency achieved by *MO*-functionalized fiber filters is due to the change in substrate chemistry caused by *MO* proteins, the removals achieved were compared to that of uncoated filters. The results showed approximately seven orders of magnitude difference in performance between *MO*-functionalized filters and uncoated filters. This clearly indicates that interactions between *MO* proteins and the model pathogens, *E. coli* and MS2, are responsible for their removal as the presence of *MO* proteins is the only difference between uncoated filters and *MO*-functionalized filters (Fig. 4a, c). The sticking coefficients of *E. coli* and MS2 empirically calculated using the experimental data and well-established models from literature (Supplementary Table 1) show that the sticking coefficient in *MO*-functionalized filters is an order of magnitude higher than in uncoated filters[28,29]. To further show that bacteria and virus tested in this study are being physically captured in *MO*-cotton filters, TEM and SEM analyses were used to visualize the MS2 and *E. coli* adhered to the surface of the cotton substrate inside *MO*-cotton filters (Fig. 4b, d). These results show that the presence of *MO*-proteins on cotton leads to an increase in the number of favorable sites for microorganism removal indicating that the presence of favorable interactions between *MO* proteins and bacteria/virus tested is responsible for their removal. Although previous literature proposed substrate modifications using polymers and nanoparticles to improve performance[10–12], *MO*-functionalized fiber filters represent a sustainable functionalization process that can be implemented easily with natural materials even in resource-limited areas.

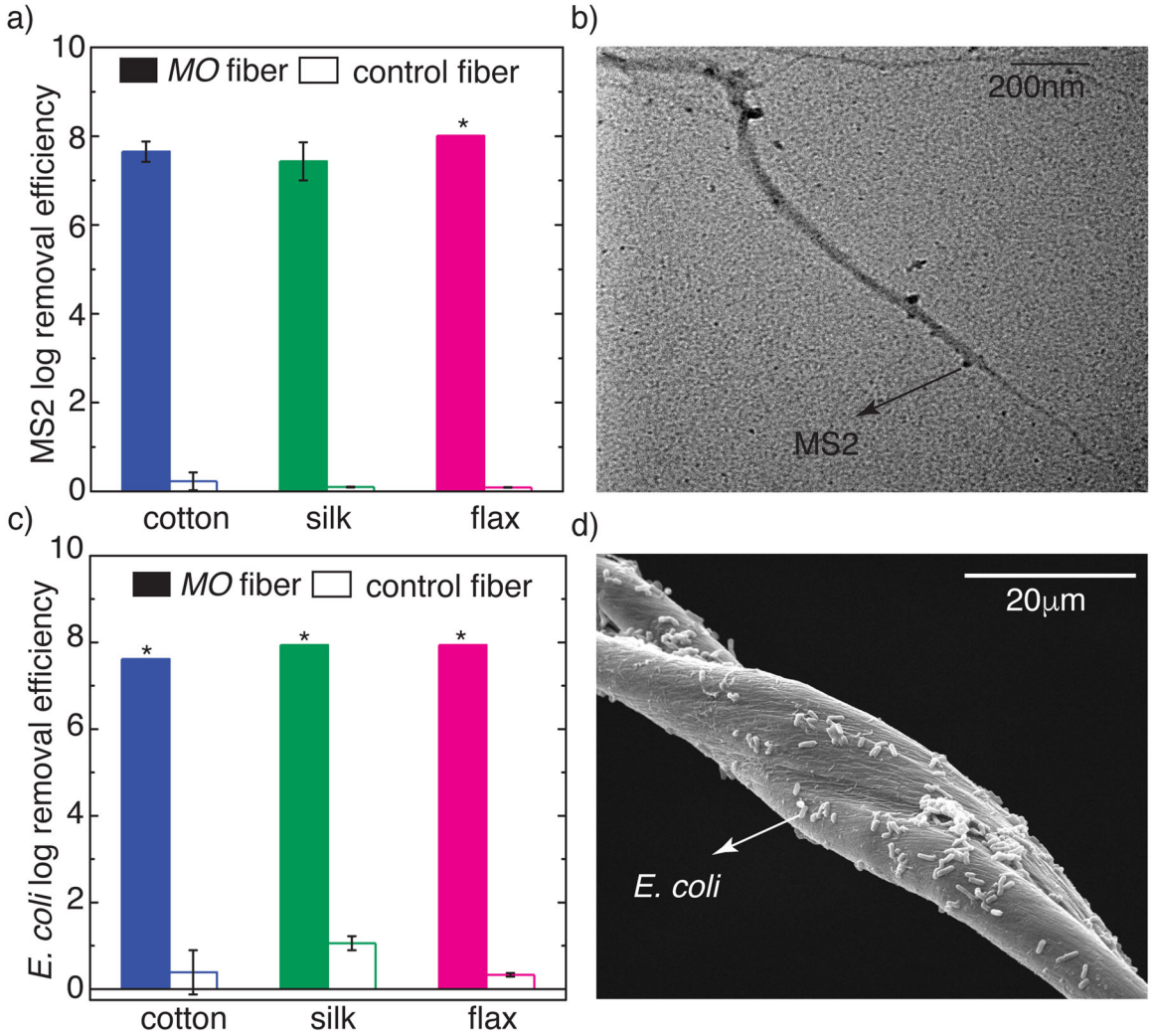

Fig. 4 ***Moringa oleifera*** **functionalized fiber filters achieve ~7 orders of magnitude higher pathogen removal compared to uncoated fiber filters indicating favorable interaction between** ***MO*** **proteins and bacteria/virus tested is responsible for their removal. a** Experimental $\log_{10}$ removal of 10^8 PFU mL^{-1} MS2 influent using *MO*-functionalized fiber filters compared to that of uncoated fiber filters at a flowrate of 2 mL min^{-1} show *MO*-fiber filters achieve ~7 orders of magnitude higher than uncoated fiber filters. **b** Transmission electron microscopy image of *MO*-cotton samples taken from a filter after filtering MS2 bacteriophage influent shows that the MS2 bacteriophage has adhered to the surface of *MO*-coated cotton. **c** Experimental $\log_{10}$ removal of 10^8 CFU mL^{-1} *E. coli* influent using *MO*-functionalized fiber filters compared to that of uncoated fiber filters at a flowrate of 2 mL min^{-1} show *MO*-fiber filters achieve >8 $\log_{10}$ removal of *E. coli* which is ~8 orders of magnitude higher than uncoated fiber filters. *Indicates that the effluent concentration was below the limit of detection which indicates that the actual removal, in this case, could be higher than the reported values. Note that flax and silk fibers used for column experiments were cleaned in boiling water to remove any impurities that can cause contamination, but this treatment did not show any significant changes in the chemical composition or morphology of the fibers (Supplementary Fig. 1). **d** Scanning electron microscopy images of uncoated cotton and *MO*-cotton samples taken from a filter after filtering *E. coli* show the adherence of the same to the surface of *MO*-cotton. All the error bars shown in the figure represent the standard deviation calculated from three independent measurements.

Surface charge analysis, column experiments at different salt concentrations, and molecular docking simulations show that removal in *MO*-cotton filters is primarily electrostatically mediated

The cationic nature of *MO* seed proteins has been established extensively in previous literature[15,17,18,30–32]. Our previous study showed that two cationic proteins, Moringa oleifera coagulant protein (MO2.1) and Moringa oleifera chitin binding protein (MoCBP) adsorb on sand particles after functionalization with a simple water extract from *MO* seed[21]. The SDS-PAGE analysis performed on the proteins adsorbed on natural fibers here (Supplementary Fig. 3) shows that the same two proteins are present on the surface of *MO*-functionalized fiber filters. The negative surface charge of both MS2 bacteriophage and *E. coli* is also well documented in literature[33–35]. We conducted separate dynamic light scattering experiments with the pathogens used in this study under the conditions used to perform filtration experiments here to confirm their negative charge. The results showed that *E. coli* and MS2 bacteriophage dispersed in 0.1XPBS and 1 mM NaCl exhibit a negative charge in a pH range of 5–8 (Supplementary Fig. 4) indicating that an attraction would exist between *E. coli*/MS2, and *MO* proteins. Therefore, the mechanism of removal in *MO*-functionalized fiber filters is based on favorable electrostatic interactions.

To further confirm this hypothesis, additional experiments were conducted to test the effect of salt concentration on the removal of MS2 bacteriophage in *MO*-cotton filters. The results clearly show that the removal of MS2 decreases with an increase in salt concentration from 1 mM to 600 mM of NaCl (Fig. 5d). Dependence on the salt concentration of the background buffer is a

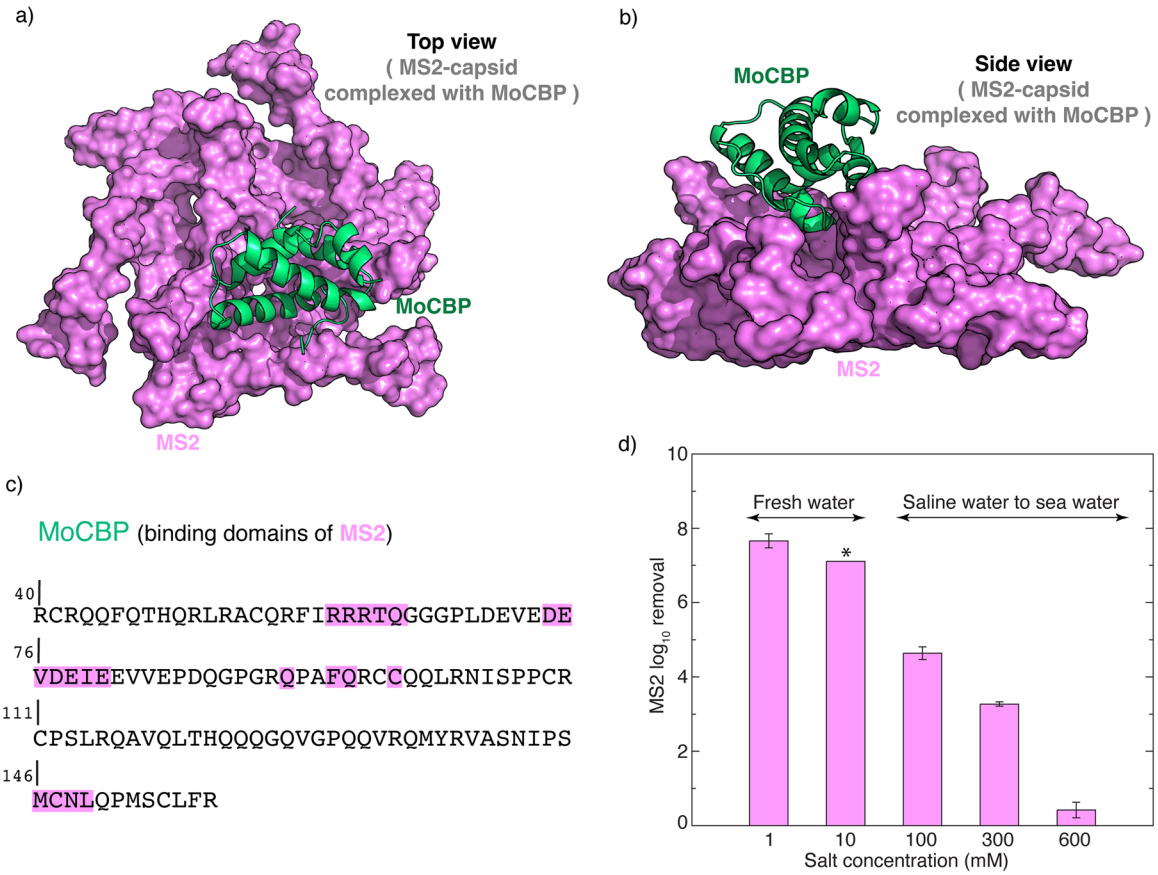

Fig. 5 Flexible molecular docking simulations and column experiments at various salt concentrations indicate that the primary mechanism of removal in *MO*-cotton filters is based on electrostatic interactions. a, **b** The top view and the side view of the favorable docking position observed from the flexible molecular docking simulations between MS2 capsid (pink) and MoCBP (green). **c** The amino acid residues that constitute the interaction interface of MS2 are overlaid onto the primary sequence of MoCBP. **d** Experimental $\log_{10}$ removal of 10^8 PFU mL^{-1} MS2 bacteriophage influent using *MO*-cotton filters at a flowrate of 2 mL min^{-1} and various salt concentrations in the range of 1–600 mM NaCl as the dispersant show the removal efficiency achieved decreases with increase in salt concentration. The $\log_{10}$ removal efficiency is based on the effluent sample collected at 50 mL effluent. *Indicates that the effluent concentration was below the limit of detection which indicates that the actual removal, in this case, could be higher than the reported values. All the error bars shown in the figure represent the standard deviation calculated from three independent measurements.

classic characteristic of electrostatic interactions. The strength of electrostatic force decreases with an increase in the buffer concentration as the Debye length decreases. These results again reiterate that the removal mechanism of *MO*-cotton filters is electrostatic in nature.

Previous work from our group explored the specific interactions between the coagulant protein from *MO* seeds (MO2.1) and *E. coli* in detail using molecular dynamics simulations and cryo-electron microscopy[15]. It was shown that MO2.1 can inactivate the bacteria by causing cell membrane fusion due to electrostatic interactions. Molecular docking simulations can be used to gain some insight into the nature of the complex interactions between virus capsid and *MO*-proteins. A detailed study of the interactions between *MO* proteins (MO2.1 and MoCBP) and MS2 bacteriophage using such simulations in our previous study showed that MoCBP is responsible for MS2 bacteriophage removal[21]. The binding interaction analysis between MoCBP and MS2 capsid protein highlighting the amino acid residues responsible for the favorable interaction and a detailed list of interactions are shown in Fig. 5a–c and Supplementary Table 2. A predominant number of interactions were found to be electrostatic interactions with cationic residues in MoCBP. A combination of all the experimental and molecular docking analyses performed suggests that the removal in *MO*-functionalized filters relies on electrostatic interactions.

MO-cotton filters offer a sustainable solution for water treatment at practically relevant superficial velocities

After the feasibility of using cotton, silk, and flax for the proposed technology was successfully shown, *MO*-cotton filters were tested to evaluate their potential to operate at practical superficial velocities. Filtration experiments at various flowrates were performed to determine the effect of flowrate on the efficiency of bacteria and virus removal. The goal was to determine the highest flowrate at which *MO*-cotton filters can meet US EPA standards for bacteria and virus treatment. The results show that *MO*-cotton filters can achieve >6 $\log_{10}$ *E. coli* removal up to 10 mL min^{-1} flowrate and >4 $\log_{10}$ MS2 removal up to 6 mL min^{-1} (Fig. 6a, b) corresponding to superficial velocities of 3.4 m h^{-1} and 2.0 m h^{-1}. The decrease in the removal efficiency with an increase in flowrate can be attributed to a decrease in the collision efficiency due to the lower residence time of pathogens in the filter[27,28]. When compared to practically relevant treatment techniques, these superficial velocities are an order magnitude higher than slow sand filtration (0.1–0.4 m h^{-1})[36] and *MO*-sand filters from our previous study[21] but only slightly lower than the

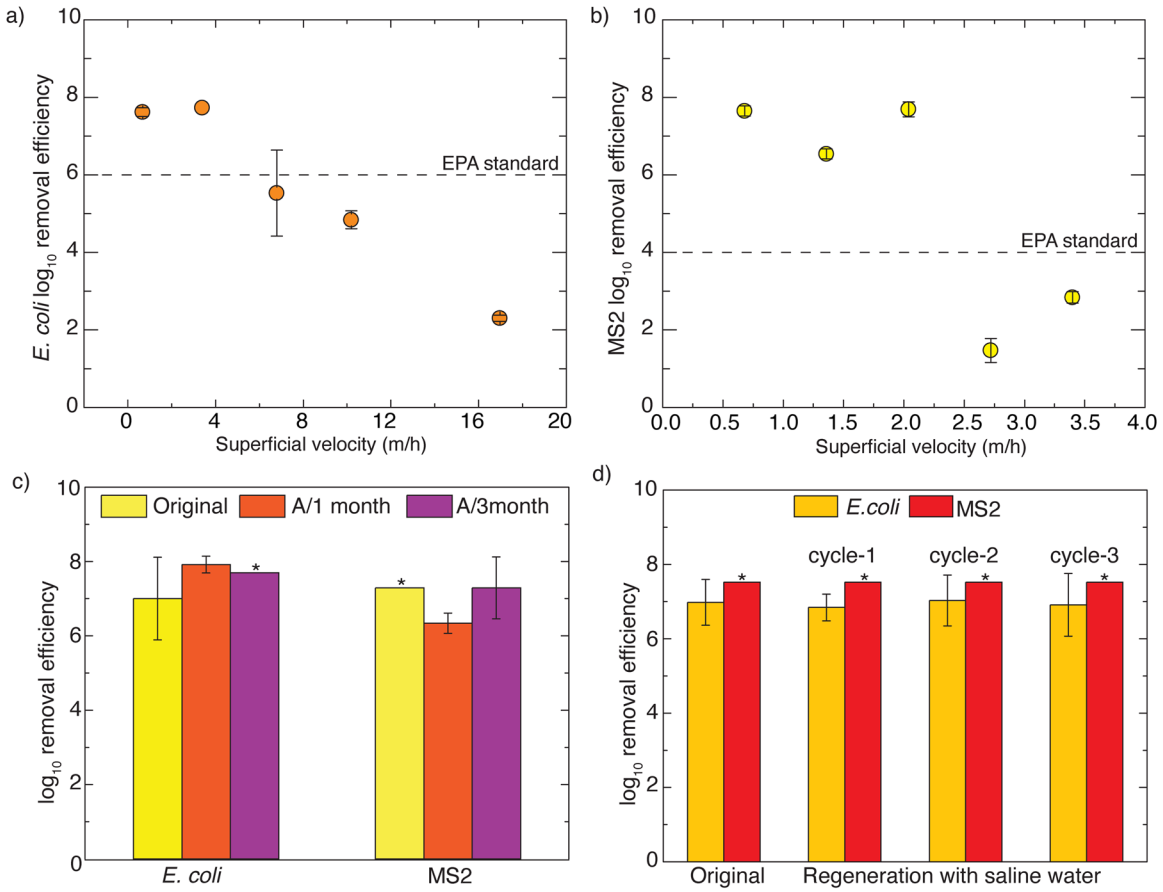

Fig. 6 *MO*-cotton filters show the potential to be a sustainable solution for virus contamination removal under practically relevant conditions for various contexts. a Experimental $\log_{10}$ removal of 10^8 CFU mL^{-1} *E. coli* influent at various flowrates in the range of 2 mL min^{-1} to 50 mL min^{-1} show that *MO*-cotton filters achieve >6 $\log_{10}$ removals up to a flowrate of 10 mL min^{-1}. **b** Experimental $\log_{10}$ removal of 10^8 PFU mL^{-1} MS2 bacteriophage influent at various flowrates in the range of 2 mL min^{-1} to 10 mL min^{-1} show that *MO*-cotton filters achieve >4 $\log_{10}$ removal up to a flowrate of 6 mL min^{-1}. These flowrates correspond to superficial velocities of 3.4 m h^{-1} and 2 m h^{-1} for *E. coli* and MS2 removal, respectively, which are slightly lower than the typical operating conditions of rapid sand filtration (5–15 m h^{-1}) and higher than slow sand filtration (0.1–0.4 m h^{-1}). **c** *E. coli* and MS2 removal efficiencies of *MO*-cotton filters at a flowrate of 2 mL min^{-1} after 1 month and 3 months of holding at room temperature. Results show that *MO*-cotton achieved 7.92 ± 0.22 $\log_{10}$ and >7.7 $\log_{10}$ removal for *E. coli* after 1 month and 3 months holding, respectively. The MS2 $\log_{10}$ removal efficiencies after 1 month and 3 months holding were 6.34 ± 0.40 and 7.29 ± 0.32. These results show that the pathogen removal efficiency of *MO*-cotton is retained until 3 months of holding. **d** *E. coli* and MS2 removal efficiency of *MO*-cotton up to 3 cycles of regeneration. The filters were regenerated by first washing with 100 mL of 600 mM NaCl solution and functionalizing with 100 mL of *MO* water extract. The removal efficiency of regenerated columns was measured at 10 mL min^{-1} for *E. coli* and 6 mL min^{-1} for MS2. It was shown that the *MO*-cotton columns remove bacteria and viruses effectively up to 3 cycles of regeneration. *Indicates that the effluent concentration was below the limit of detection which indicates that the actual removal, in this case, could be higher than the reported values. Error bars represent the standard deviation calculated from three independent measurements.

typical superficial velocities in rapid sand filtration (5–15 m h^{-1})[37]. As discussed earlier, *MO*-cotton filters offer smaller mean pore size and higher surface areas compared to sand filters from previous work. We believe a combination of these properties offers advantages in terms of the amount of protein adsorbed per filter and thus higher overall capacity for virus removal.

Further experiments were performed to estimate the dry holding stability and capability of regenerating *MO*-cotton to consider the sustainability and ease of accessibility for various contexts. Previous studies show that transmission of infectious disease is widespread after natural disasters due to the lack of clean water[38]. If *MO*-cotton exhibits dry storage stability, it can be applied to water treatment in disaster relief situations to prevent disease spread by shipping pre-made *MO*-cotton to the affected areas or storage in emergency preparedness kits. The experiments conducted to study dry storage stability showed that dried *MO*-cotton retains the ability to filter bacteria and viruses from water for up to 3 months at room temperature. *E. coli* and MS2 removal achieved by *MO*-cotton retrieved from storage after 1 month and 3 months is similar to freshly prepared *MO*-cotton (Fig. 6c). Although cotton is a biodegradable material, regeneration capability is important for *MO*-cotton to be a sustainable substrate. To test regeneration capability, experiments were conducted using 600 mM NaCl to desorb the protein before recoating with *MO* water extract to show *in-situ* regeneration of the filter upon breakthrough. The inspiration for this regeneration process was based on previous literature which showed that 600 mM NaCl could be successfully used to desorb *MO* proteins from silica surfaces[31]. Results showed that bacteria and virus removal efficiency after regeneration is similar to the freshly prepared *MO*-cotton, up to 3 cycles of regeneration (Fig. 6d). Note that regeneration here is different from the physical backwash used for conventional sand filters on an hourly to daily basis in the water treatment plants. The current filter could be easily backwashed without losing effectiveness. These results show that *MO*-cotton can be a sustainable substrate for water treatment in various contexts including disaster relief situations and ready-made point-of-use filtration.

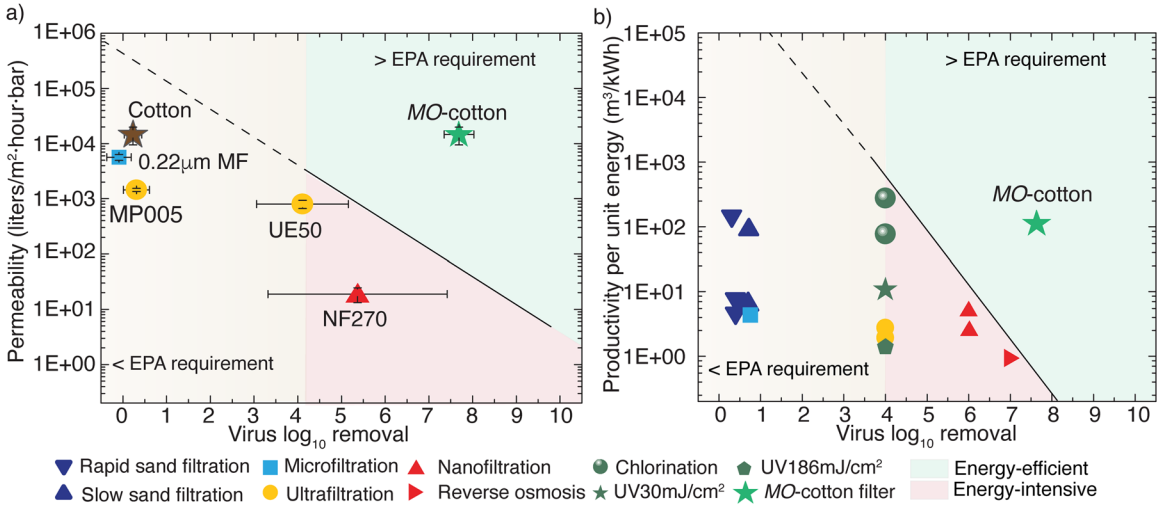

Fig. 7 *MO*-cotton filters show potential for an energy-efficient solution for virus contamination removal compared to commercially available membrane filters. a The MS2 log removal efficiency of various membrane filters tested in this work was compared to that of uncoated and coated cotton filters proposed in this study to show the advantage of *MO* functionalization. The experimental permeability and MS2 removal efficiency values determined for the tested commercial membranes and *MO*-cotton filters are available in Supplementary Table 7. **b** Preliminary assessment of energy requirement for a theoretical point-of-use *MO*-cotton filter shows the energy required is much lower compared to membrane filtration and UV irradiation. The energy requirement for *MO*-filters is on par with conventional media filtration and chlorine disinfection. The energy requirement of various techniques shown in this figure is based on available literature and a detailed summary of the literature survey and energy requirement values used can be found in Supplementary Note 2 and Supplementary Table 5. All the error bars shown in the figure represent the standard deviation calculated from three independent measurements.

MO-cotton filters are a low energy-intensity virus removal solution

Traditional filtration techniques based on size-exclusion in the context of water filtration are limited by the existence of a trade-off between their productivity and pathogen removal. This trade-off was shown experimentally, for the first time, by characterizing MS2 bacteriophage removal of microfiltration (MF), ultrafiltration (UF), and nanofiltration (NF) membranes with controlled experiments. The MS2 removal efficiency and permeability of commercially available MF, UF, and NF membranes were studied in a dead-end filtration setup at constant pressure required to maintain a flowrate of approximately 100 LMH (liter·m^{-2}·h^{-1}) (Fig. 7a). This trade-off curve was established to add a perspective to the advantage of molecularly redesigning conventional water filters with *MO* protein functionalization. The results indicate that functionalizing the surface of an uncoated cotton filter with *MO* proteins is a sustainable way of increasing the performance by orders of magnitude without any decrease in the inherent permeability, thus overcoming the productivity-permeability limit of current filtration approaches (Fig. 7b). This shows the potential of the filters proposed in this study as an energy-efficient and accessible water filtration technique that can be applied to water treatment in both developing and developed countries.

In the current work, the primary focus was to establish the feasibility of *MO*-functionalized fiber filters for achieving high virus removal at high loading rates. Although future scale-up studies at realistic conditions are necessary for a comprehensive life cycle analysis, an initial assessment of energy requirement for *MO*-cotton filters was performed here to compare the proposed filters with alternative virus removal technologies. The detailed analysis for calculation of the operational and embodied energy required for a theoretical point-of-use *MO*-cotton filter is available in Supplementary Note 1. The analysis showed that *MO*-cotton filters require minimal energy when compared to alternative techniques (Fig. 7b). The low energy requirement of *MO*-cotton filters (0.01kWh m^{-3}) is similar to less energy-intensive technologies such as conventional media filtration and chlorine disinfection. Compared to the energy-intensive alternatives of membrane filtration and UV irradiation, *MO*-cotton filters show potential for energy-efficient virus treatment. This shows that *MO*-cotton filters have great promise as an easily accessible drinking water filter that can be deployed as a point-of-use filter or a community scale filter in the future. In addition to the energy consumption, the cost for building the proposed theoretical point-of-use design of *MO*-cotton filter in both the USA and India was calculated based on the material costs from our experience with setting up filters in the field at two locations (Supplementary Fig. 7). These estimates showed that a point-of-use *MO*-cotton filter with a capacity of filtering 10 liters of water per day costs $10 and $5 per filter to fabricate in USA and India, respectively (details in Supplementary Note 3 and Supplementary Table 6).

DISCUSSION

Overall, we have demonstrated that a simple aqueous *Moringa oleifera* seed extract can be used effectively to functionalize easily-accessible natural fibers and show how the proposed filters can overcome a trade-off curve that exists in size-exclusion filtration techniques. A regeneration method was developed and the dry-storage stability of *MO*-cotton was studied to establish its potential as a sustainable technique applicable to various contexts. Finally, it was shown with experiments and preliminary energy estimation that the proposed filters offer highly efficient virus removal capability with low-energy requirement compared to commercially available membranes. Even though the findings from this laboratory-scale study are encouraging, to adapt the proposed filters at the field scale, future work needs to focus on the effect of practical conditions on filter performance. Important parameters to consider include the pressure required to operate the column and realistic pathogen concentrations in the presence of organic matter. In the field, these filters are designed to be driven by gravity-assisted flow. The experiments shown here were conducted at a constant flowrate using a peristaltic pump because the pressure required for maintaining a flow of 2 mL min^{-1} is less than 1 psi and it is difficult to maintain and measure such a low pressure reliably. A constant pressure setup was used to quantify the permeability (flowrate per unit area per unit pressure) of

MO-cotton filters and compared this to conventional membranes (Fig. 7a). These results indicate very high permeability for *MO*-functionalized filters but field-scale experiments are necessary to validate this data further.

Secondly, the goal of the experiments performed here was to quantify the highest efficiency achievable by *MO*-cotton filters compared to uncoated filters at 'clean-bed' conditions by filtering a relatively low volume of high concentration bacteria/virus solution. In practice, high volumes of water with pathogen concentrations orders of magnitude lower than that used in the current work will be processed. Separate breakthrough experiments were performed with *E. coli* to establish a preliminary estimate of the life of a *MO*-cotton filter and the effect of natural organic matter on capacity. These experiments showed that (Supplementary Fig. 5a) *MO*-cotton filters remove $>10^{11}$ colony forming units (CFU) of bacteria before reaching saturation. This translates to $>10^7$ column volumes for even a heavily-contaminated source water (100 CFU mL^{-1} of bacteria) indicating the high capacity of *MO*-cotton filters. The filters also did not show any susceptibility to biofouling during this long-term experiment. The estimate of a lifetime from laboratory experiments is expected to decrease in field applications due to the complex composition of natural water. To understand the effect of the water matrix, pond water containing high total organic carbon (TOC ~6 mg mL^{-1}) spiked with *E. coli* was tested with *MO*-functionalized sand filters. The results show that the column capacity decreases approximately by half due to the effect of TOC (Supplementary Fig. 5b). As the pond water used for this preliminary experiment was collected from a local water source, accurate determination of the composition of natural organic matter was not possible. A detailed study with a careful variation of concentrations and composition of natural organic matter (NOM) considering the available pre-filter and pre-treatment options for the removal of NOM is an important future area of inquiry.

METHODS

Moringa oleifera seeds

The *Moringa oleifera (MO)* seeds used for this study were received from Echo Global farm, Florida. The dried *MO* seeds were stored in a sealed bag at room temperature and crushed with a coffee grinder before the experiment. These conditions were intentionally used to ensure the process is robust under the storage and coating conditions that can be easily followed in field applications. Column experiments were performed with freshly made water extract to establish the removal efficiency of functionalized fiber filters.

Natural fibers

The details of the natural fibers used are available in Supplementary Methods.

Commercial flat sheet membranes

NF270 (PA-TFC, Dow Filmtec), UE50 (PES, Trisep), and MP005 (PES, Microdyn Nadir) purchased from the Sterlitech Corporation were used for determining the permeability and MS2 removal efficiency of nanofiltration (NF), tight ultrafiltration (UF), and loose UF, respectively. The 0.22 µm (PVDF, Millipore™) membrane purchased from Millipore Sigma was used as an example of a microfiltration membrane.

Microorganisms for filtration experiments

Two microorganisms were used in this study to challenge the *MO*-functionalized fiber filters and quantify their removal efficiency: *Escherichia coli* TG1 strain and MS2 bacteriophage. *E. coli* is a rod-shaped gram-negative bacillus, typically 1 µm long and 0.35 µm wide, that has been used ubiquitously as a model organism in scientific research[39]. The *E. coli* TG1 strain used in this study was shown to be an effective surrogate for bacteria in our previous studies[22,40]. MS2 bacteriophage is a nonenveloped single-stranded RNA coliphage, 27 nm in diameter, that has been used widely as a surrogate for human enteric viruses[26,41]. These model microorganisms were used to challenge the filters in this study as they are ideal surrogates to represent bacteria and virus particles due to their size. In addition, they also pose lower risks of associated infection and are easier to culture and quantify rapidly. The procedure for *E. coli* TG1 and MS2 propagation and culture are detailed in Supplementary Methods.

Moringa oleifera (MO) functionalized fiber filter preparation

Readily available components were used to build the column filters used to quantify the pathogen removal in this study. Glass chromatography columns with dimensions of 1.5 cm inner diameter and 10 cm length, manufactured by Bio-Rad, were used as the filter body to pack the fiber. First, six balls (~3.5 gm) of cotton, 5 gm of silk fiber, or 8 gm of flax fiber were soaked in water for 2 min. Although DI water is used here, any clean water would work for this step. The wet fiber was pushed into the column using a plunger. The dry weight of the fiber that was packed in each column and the height of the column was measured to account for the inherent variation in the size and weight of the individual cotton balls. The average heights of cotton, silk, and flax fiber columns were ~8 cm, ~8.2 cm, and ~9.5 cm, respectively.

To functionalize the thus prepared fiber filter with *MO* proteins, 100 mL of water extract from dry *MO* seeds was pumped through the column at a constant flowrate of 2 mL min^{-1}. *MO* water extract is prepared by mixing 2 gm of freshly ground unshelled *MO* seed with 100 mL DI water for 5 min. Although DI water was used here for preparing the *MO* serum extract, the presence of 10 mM NaCl did not show any significant effect on the performance of *MO*-functionalized filters (Supplementary Fig. 6). This solution was filtered sequentially through a 1.5 µm glass fiber filter (Whatman) and 0.22 µm PVDF filter (Millipore), to remove excess seed material before using it to functionalize the fiber filters.

Membrane testing with MS2 bacteriophage to compare the performance of *MO*-cotton

Membrane filtration of MS2 bacteriophage was performed in a 10 mL dead-end filtration setup (Model 8010, Millipore) with an active membrane area of 4.1 cm^2. The filtration cell was connected to an 800 mL Amicon Stirred Cell Reservoir plastic reservoir (RC800, Millipore) to continuously feed at a stirring rate of 300 RPM. The filtration rate for each membrane was maintained at ~100 LMH (liters m^{-2} h^{-1}) by adjusting applied pressure to achieve a comparable flowrate to the column performance. The feed and permeate were collected after filtering 200 mL of the feed solution. This procedure is widely used in literature to quantify the performance of membranes[42,43].

Quantification of pathogen removal

A series of standard filtration experiments were used to quantify the pathogen removal efficiency of *MO*-functionalized fiber filters in this study. After preparing a *MO*-functionalized filter according to the procedure in the prior section, the filter was equilibrated with 100 mL of the background buffer at the required flowrate for the filtration experiment. Unless specified otherwise, the background buffer used in this study for *E. coli* was 10 times diluted PBS buffer (0.1X PBS) and for MS2 bacteriophage was 1 mM NaCl solution. For the column experiments performed to infer the mechanism of MS2 removal in *MO*-cotton filters, the background salt concentration was varied in the range of 1–600 mM NaCl (10 mM, 100 mM, 300 mM, and 600 mM). After equilibration, an influent solution containing either ~10^8 CFU mL^{-1} of *E. coli* or ~10^8 PFU mL^{-1} of MS2 bacteriophage dispersed in the background buffer was fed to the filter at a constant flowrate. Three effluent samples were collected when 50 mL, 75 mL, and 100 mL of the influent had passed through the filter. Experimental log removal efficiency (LRE) of the filters was quantified using Eq. 1, where C and C_0 represent the effluent and influent sample concentrations. The concentration of the viable pathogens in influent and effluent samples was quantified using a conventional plating technique for *E. coli* and a double layer plaque assay for MS2 bacteriophage. The details of the quantification techniques used can be found in Supplementary Methods.

$$\log \text{removal efficiency}(\text{LRE}) = -\log_{10}\left[\frac{C}{C_0}\right] \quad (1)$$

To quantify the efficiency of functionalizing fibers with *MO* proteins in enhancing the pathogen removal, filtration experiments were performed at a flowrate of 2 mL min^{-1} using *MO*-functionalized fiber filters. Uncoated

fiber filters packed and processed using the same procedure as a *MO*-functionalized filter, except for the functionalization step, were used as a negative control. To understand the effect of flowrate on the LRE, experiments were performed using *MO*-functionalized cotton filters at varying flowrates in the range of 2 mL min^{-1} to 50 mL min^{-1} for *E. coli* and 2 mL min^{-1} to 10 mL min^{-1} for MS2 bacteriophage.

Molecular docking simulations

In order to quantify the binding affinity between MoCBP and MS2 capsid proteins, a series of flexible docking iterations were performed scanning the surface of the target capsids using the surface docking protocol of OptMAVEn-2.0[44] which is similar to Z-DOCK-3[45]. Coordinates of the center of mass of the top 100 docked conformations of MoCBP were used to identify the highest MoCBP-affinity location(s) on the capsid proteins. For each of the bound conformations of MoCBP at the high-affinity region, an all-atom Rosetta energy function was used to estimate the enthalpic contribution of binding. Input file preparation involved starting with the crystallographic coordinates of each of the proteins involved – (a) MoCBP – PDB id 5DOM[32], (b) MS2 capsid – PDB id 1AQ3[46] – and then subsequently performing an internal coordinate building to add any missing residues and overall energy minimization using the all-atom relaxation protocol *Relax* within PyRosetta[47].

Experiments to test dry holding stability of *MO*-cotton

It is important for *MO*-functionalized cotton (*MO*-cotton) to retain its ability to capture pathogens after drying and holding for a long time, for the proposed technique to be applicable under varied contexts (e.g., disaster preparedness). To test this, *MO*-cotton prepared according to the procedure mentioned before was dried at 37 °C for 24 h and stored in a sealed bag at room temperature. Then filtration experiments were performed with the dry *MO*-cotton after 1 month and 3 months to compare the LRE with freshly coated cotton. Note that 1-month and 3-month samples were taken from identical batches of *MO*-cotton prepared on the same day and left for drying at room temperature in a sealed bag. Filtration experiments were performed following the same procedure as above at a flowrate of 2 mL min^{-1}.

Regeneration of *MO*-cotton

To show that *MO*-cotton is a widely available and sustainable pathogen capture media, it is important to establish the capability of regenerating the coated cotton easily. Our previous studies have shown that washing with a 600 mM saline solution followed by functionalization with *MO* water extract is an effective procedure to regenerate filtration media[21,31]. To check if a similar procedure can be used to regenerate *MO*-cotton, filtration experiments were performed to determine the effect of regeneration on pathogen removal efficiency. *MO*-cotton columns were first prepared according to the procedure described before and then washed with 100 mL of 600 mM NaCl to desorb the protein before re-coating them. This process was repeated three times, and the *E. coli* and MS2 removal efficiency of the regenerated columns were quantified for each cycle to study the effect of regeneration on LRE.

Surface area measurement

Brunauer–Emmett–Teller (BET) isotherm measurements were used to analyze the surface available of different fibers used in this study. Three samples per fiber (cotton, silk, and flax) were submitted for analysis at The Material Characterization Lab at The Pennsylvania State University to determine the average available surface area (SA). SA was determined by the physical adsorption of nitrogen on a sample surface at 77 K using Accelerated Surface Area and Porosimetry Analyzer (ASAP 2420; Micromeritics Instrument Corp.). SA was calculated using BET equation[48] which utilizes the linear part of the adsorption isotherm at relative pressures, P/P_o, in the range between 0.05 and 0.30, where P is the equilibrium pressure and P_o is the saturation pressure. Prior to the measurement, samples were degassed at 40 °C for at least 8 h under a vacuum of 4 µm Hg to remove impurities such as water vapor, carbon dioxide, and others.

FTIR analysis

Attenuated total reflectance Fourier transform infrared spectroscopy (ATR-FTIR) was performed on the fiber samples to determine their chemical structures using Nicolet 6700 spectrometer (Thermo Scientific) with smart iRT diamond ATR sampling accessory (Thermo Scientific). 256 scans per sample at a resolution of 4 cm^{-1} were obtained for all measurements.

Streaming potential analysis

To measure the surface potential of the fiber samples, a SurPASS electrokinetic analyzer (Anton Paar, Ashland, VA, USA) was used. Each fiber sample was first soaked in 10 mL of 1 mM NaCl solution. Then the sample was mounted within the cylindrical cell on the device and pH of the electrolyte solution (again 1 mM NaCl) was adjusted to the required level using 0.05 M HCl and NaOH. Measurements were made in triplicate for each fiber at four different pH values of 5, 6, 7, and 8. All the measurements were made at a target pressure of 300 mBar. Note that this pressure is an operational requirement for the electrokinetic analyzer and does not have any correlation to the operating pressure of the filtration experiments in this study.

Capillary flow porometry

To measure the mean pore size of the fiber columns tested in this study, required amount of the fiber sample was packed in a cylindrical holder with dimensions of 2.54 cm length and 3.5 cm diameter to reach a packing density of cotton, silk, and flax similar to the column filters. Water was used as the wetting liquid and porometry analysis was performed using the standard wet-up and calc. dry measurement protocol in an iPore 1100-AX from Porous Materials Inc. The term column packing density used in this context does not represent bulk density or the porosity of the fiber in the filter. Instead, it is the ratio of the amount of material packed over the volume of the column and is meant to be a reference value to enable comparison in future studies.

Quantitative and Qualitative analysis of adsorbed MO protein

To determine the amount of protein adsorbed on the natural fiber filters, a Thermo Scientific™ Pierce™ Quantitative Fluorescent Peptide Assay was used. Lysozyme from chicken egg white was used to develop a calibration curve. After coating the column as explained earlier, 100 mL of 600 mM NaCl was introduced at a flowrate of 2 mL min^{-1} to desorb the protein into the salt solution[31]. The concentration of the protein in the salt solution was used to interpret the amount of the *MO* protein adsorbed onto the surface of a fiber filter.

To qualitatively characterize the protein adsorbed on the surface of natural fibers, Sodium Dodecyl Sulfate- Poly- Acrylamide Gel Electrophoresis[49] (SDS-PAGE) evaluation was conducted on the salt wash used to quantify the adsorbed protein. 12 µL of 600 mM NaCl wash was loaded onto a 12% hand-cast SDS PAGE gel. Coomassie staining was used to visualize the protein bands.

Transmission electron microscopy

Transmission electron microscopy (TEM) was used for observing the MS2 bacteriophage physically removed using *MO*-cotton filters. To visualize the MS2 bacteriophage attached to *MO*-cotton, a negative-stain method was used with TEM analysis. The *MO*-cotton fiber with adsorbed MS2 bacteriophage was prepared by filtering 4000 mL of 10^8 PFU mL^{-1} MS2 bacteriophage dispersed in 1 mM NaCl with a *MO*-cotton filter at 6 mL min^{-1}. Individual fibers from the top of the column were picked with a clean tweezer and dried either at 35 °C or using hexamethyldisilazane (HMDS) drying for the imaging analysis.

To preserve and chemically fix the specimen's structure, a chemical drying agent HMDS was used to dehydrate soft tissues and biological molecules prior to the TEM examination. The specimens to be examined were dehydrated through varying concentrations of graded ethanol (30%, 50%, 60%, 70%, 80%, 90%, and 100% ethanol) for 10 min each and then maintained in 50% ethanol/HMDS and 100% HMDS for 2 min each in succession at room temperature. The specimens were then dried overnight in a laminar flow hood. The dehydrated specimens were adsorbed onto 400-mesh, glow-discharged, carbon-coated TEM grids (G400, Ted Pella) and negatively stained with 0.75% (w v^{-1}) uranyl formate. TEM images were obtained on the Tecnai G2 Spirit BioTwin microscope (FEI) at an accelerating voltage of 80 kV. Images were taken at a magnification between 6 kx to 87 kx using an AMT Advantage HR 1k X 1k digital camera (Advanced Microscopy Techniques).

Scanning electron microscopy

Scanning electron microscopy (SEM) was used in this study to observe the adsorption of *E. coli* on the surface of *MO*-cotton fiber. SEM was also used to analyze the fiber diameter and morphologies of cotton, silk, and flax fibers used in this study before and after treating with boiled water for 15 min to understand the effect of treatment on morphology. The *MO*-cotton fiber with adsorbed *E. coli* bacteria was prepared by filtering 2000 mL of 10^8 CFU mL^{-1} *E. coli* dispersed in 0.1X PBS with a *MO*-cotton filter at 10 mL min^{-1}. Individual fibers from the top of the column were picked with clean tweezer and dried using HMDS drying for the imaging analysis.

To preserve and chemically-fix the structure of the biological specimen, HMDS drying technique detailed earlier was used to dehydrate soft tissues and biological molecules prior to the examination by SEM for natural fiber samples treated with boiled water and *MO*-cotton with *E. coli*. Once the samples were prepared, SEM images were acquired using Quanta 650 ESEM (FEI) at an acceleration voltage of 5 kV to 15 kV, and specimens were coated with a gold/palladium mixture using EMS Sputter Coater to prevent static charge accumulation.

DATA AVAILABILITY

The datasets that support the finding of this study are available in the Texas Data repository at https://doi.org/10.18738/T8/BKRUCG. It is also available on Zenodo at https://doi.org/10.5281/zenodo.6607398

Received: 4 December 2021; Accepted: 10 June 2022;
Published online: 06 July 2022

REFERENCES

1. Hochella, M. F. et al. Natural, incidental, and engineered nanomaterials and their impacts on the Earth system. *Science* **363,** eaau8299 (2019).
2. Bouseettine, R., Hassou, N., Bessi, H. & Ennaji, M. M. in *Emerging and Reemerging Viral Pathogens* 907–932 (Elsevier, 2020).
3. Shirasaki, N., Matsushita, T., Matsui, Y. & Yamashita, R. Evaluation of the suitability of a plant virus, pepper mild mottle virus, as a surrogate of human enteric viruses for assessment of the efficacy of coagulation–rapid sand filtration to remove those viruses. *Water Res.* **129**, 460–469 (2018).
4. Organization, W. H. Drinking water parameter cooperation project. *Support Revis. Annex I Counc. Directive* **98**, 83 (2017).
5. Yahya, M., Cluff, C. & Gerba, C. Virus removal by slow sand filtration and nanofiltration. *Water Sci. Technol.* **27**, 445–448 (1993).
6. ElHadidy, A. M., Peldszus, S. & Van Dyke, M. I. An evaluation of virus removal mechanisms by ultrafiltration membranes using MS2 and φX174 bacteriophage. *Sep. Purif. Technol.* **120**, 215–223 (2013).
7. Chen, S. & Chen, B. Urban energy–water nexus: a network perspective. *Appl. Energy* **184**, 905–914 (2016).
8. Richardson, S. D., Plewa, M. J., Wagner, E. D., Schoeny, R. & DeMarini, D. M. Occurrence, genotoxicity, and carcinogenicity of regulated and emerging disinfection by-products in drinking water: a review and roadmap for research. *Mutat. Res Rev. Mutat. Res* **636**, 178–242 (2007).
9. Mo, W., Cornejo, P. K., Malley, J. P., Kane, T. E. & Collins, M. R. Life cycle environmental and economic implications of small drinking water system upgrades to reduce disinfection byproducts. *Water Res.* **143**, 155–164 (2018).
10. Szekeres, G. P. et al. Copper-coated cellulose-based water filters for virus retention. *ACS omega* **3**, 446–454 (2018).
11. Zodrow, K. et al. Polysulfone ultrafiltration membranes impregnated with silver nanoparticles show improved biofouling resistance and virus removal. *Water Res.* **43**, 715–723 (2009).
12. Sinclair, T. et al. Virus reduction through microfiltration membranes modified with a cationic polymer for drinking water applications. *Colloids Surf. Physicochem. Eng. Asp.* **551**, 33–41 (2018).
13. Palika, A. et al. An antiviral trap made of protein nanofibrils and iron oxyhydroxide nanoparticles. *Nat. Nanotechnol.* **16.8**, 918–925 (2021).
14. Ndabigengesere, A., Narasiah, K. S. & Talbot, B. G. Active agents and mechanism of coagulation of turbid waters using Moringa oleifera. *Water Res.* **29**, 703–710 (1995).
15. Shebek, K. et al. The flocculating cationic polypetide from Moringa oleifera seeds damages bacterial cell membranes by causing membrane fusion. *Langmuir* **31**, 4496–4502 (2015).
16. Fuglie, L. J. The Miracle Tree: Moringa oleifera: Natural Nutrition for the Tropics. Church World Service, Dakar. 68 p; revised in 2001 and published as The Miracle Tree: The Multiple Attributes of Moringa, 172 p (1999).
17. Gifoni, J. M. et al. A novel chitin-binding protein from Moringa oleifera seed with potential for plant disease control. *Pept. Sci.* **98**, 406–415 (2012).
18. Neto, J. X. et al. A chitin-binding protein purified from Moringa oleifera seeds presents anticandidal activity by increasing cell membrane permeability and reactive oxygen species production. *Front. Microbiol.* **8**, 980 (2017).
19. Foidl, N., Makkar, H. & Becker, K. The potential of Moringa oleifera for agricultural and industrial uses. *What development potential for Moringa products* **20** (2001).
20. Ferreira, P. M. et al. Larvicidal activity of the water extract of Moringa oleifera seeds against Aedes aegypti and its toxicity upon laboratory animals. *Acad. Bras. Cienc.* **81**, 207–216 (2009).
21. Samineni, L. et al. 7 log virus removal in a simple functionalized sand filter. *Environ. Sci. Technol.* **53**, 12706–12714 (2019).
22. Xiong, B. et al. Moringa oleifera f-sand Filters for Sustainable Water Purification. *Environ. Sci. Technol. Lett.* **5**, 38–42 (2018).
23. Brown, P. & Cox, C. L. *Fibrous filter media*. (Woodhead Publishing, 2017).
24. Peets, P., Kaupmees, K., Vahur, S. & Leito, I. Reflectance FT-IR spectroscopy as a viable option for textile fiber identification. *Herit. Sci.* **7**, 1–10 (2019).
25. Blaustein, R., Pachepsky, Y., Hill, R., Shelton, D. & Whelan, G. Escherichia coli survival in waters: temperature dependence. *Water Res.* **47**, 569–578 (2013).
26. Aranha-Creado, H. & Brandwein, H. Application of bacteriophages as surrogates for mammalian viruses: a case for use in filter validation based on precedents and current practices in medical and environmental virology. *PDA J. Pharm. Sci. Technol.* **53**, 75–82 (1999).
27. Logan, B., Jewett, D., Arnold, R., Bouwer, E. & O'Melia, C. Clarification of clean-bed filtration models. *J. Environ. Eng.* **121**, 869–873 (1995).
28. Tufenkji, N. & Elimelech, M. Correlation equation for predicting single-collector efficiency in physicochemical filtration in saturated porous media. *Environ. Sci. Technol.* **38**, 529–536 (2004).
29. Logan, B. E., Hilbert, T. A. & Arnold, R. G. Removal of bacteria in laboratory filters: models and experiments. *Water Res.* **27**, 955–962 (1993).
30. Ghebremichael, K. A., Gunaratna, K., Henriksson, H., Brumer, H. & Dalhammar, G. A simple purification and activity assay of the coagulant protein from Moringa oleifera seed. *Water Res.* **39**, 2338–2344 (2005).
31. Nordmark, B. A. et al. Moringa oleifera seed protein adsorption to silica: effects of water hardness, fractionation, and fatty acid extraction. *Langmuir* **34**, 4852–4860 (2018).
32. Ullah, A. et al. Crystal structure of mature 2S albumin from Moringa oleifera seeds. *Biochem. Biophys. Res. Commun.* **468**, 365–371 (2015).
33. Morrow, J., Stratton, R., Yang, H.-H., Smets, B. F. & Grasso, D. Macro-and nanoscale observations of adhesive behavior for several E. coli strains (O157: H7 and environmental isolates) on mineral surfaces. *Environ. Sci. Technol.* **39**, 6395–6404 (2005).
34. Bolster, C., Haznedaroglu, B. & Walker, S. Diversity in cell properties and transport behavior among 12 different environmental Escherichia coli isolates. *J. Environ. Qual.* **38**, 465–472 (2009).
35. Armanious, A. et al. Viruses at solid–water interfaces: a systematic assessment of interactions driving adsorption. *Environ. Sci. Technol.* **50**, 732–743 (2016).
36. Crittenden, J. C. et al. MWH's water treatment: principles and design. John Wiley & Sons (2012).
37. Ellis, K. V. & Wood, W. E. Slow sand filtration. *Crit. Rev. Environ. Control* **15**, 315–354, https://doi.org/10.1080/10643388509381736 (1985).
38. Kouadio, I. K., Aljunid, S., Kamigaki, T., Hammad, K. & Oshitani, H. Infectious diseases following natural disasters: prevention and control measures. *Expert Rev. Anti Infect. Ther.* **10**, 95–104 (2012).
39. Chen, X. et al. Metabolic engineering of Escherichia coli: a sustainable industrial platform for bio-based chemical production. *Biotechnol. Adv.* **31**, 1200–1223 (2013).
40. Wood, T. L. et al. Living biofouling-resistant membranes as a model for the beneficial use of engineered biofilms. *Proc. Natl Acad. Sci. USA* **113**, E2802–E2811 (2016).
41. Amarasiri, M., Kitajima, M., Nguyen, T. H., Okabe, S. & Sano, D. Bacteriophage removal efficiency as a validation and operational monitoring tool for virus reduction in wastewater reclamation. *Water Res.* **121**, 258–269 (2017).
42. Wickramasinghe, S. R., Stump, E. D., Grzenia, D. L., Husson, S. M. & Pellegrino, J. Understanding virus filtration membrane performance. *J. Membr. Sci.* **365**, 160–169 (2010).
43. Tu, Y.-M. et al. Rapid fabrication of precise high-throughput filters from membrane protein nanosheets. *Nat. Mater.* **19**, 347–354 (2020).
44. Chowdhury, R., Allan, M. F. & Maranas, C. D. OptMAVEn-2.0: de novo design of variable antibody regions against targeted antigen epitopes. *Antibodies* **7**, 23 (2018).

45. Pierce, B. G., Hourai, Y. & Weng, Z. Accelerating protein docking in ZDOCK using an advanced 3D convolution library. *PLoS One* **6**, e24657 (2011).
46. van den Worm, S. H. et al. Crystal structures of MS2 coat protein mutants in complex with wild-type RNA operator fragments. *Nucleic Acids Res.* **26**, 1345–1351 (1998).
47. Nivón, L. G., Moretti, R. & Baker, D. A Pareto-optimal refinement method for protein design scaffolds. *PLoS One* **8**, e59004 (2013).
48. Brunauer, S., Emmett, P. H. & Teller, E. Adsorption of gases in multimolecular layers. *J. Am. Chem. Soc.* **60**, 309–319 (1938).
49. Weber, K. & Osborn, M. The reliability of molecular weight determinations by dodecyl sulfate-polyacrylamide gel electrophoresis. *J. Biol. Chem.* **244**, 4406–4412 (1969).
50. Gaspar, D. et al. Nanocrystalline cellulose applied simultaneously as the gate dielectric and the substrate in flexible field effect transistors. *Nanotechnology* **25**, 094008 (2014).
51. Yang, M.-H. et al. Characterization of silk fibroin modified surface: a proteomic view of cellular response proteins induced by biomaterials. *Biomed Res. Int.* **2014**, https://doi.org/10.1155/2014/209469 (2014).

ACKNOWLEDGEMENTS

The authors would like to thank Echo Global Farm, Florida for providing *Moringa oleifera* seeds. The authors acknowledge Dr. Katya Bazilevskaya for the help in preparation of samples and analysis of surface area using BET measurements. The authors would like to thank Dr. Tammy Wood for providing the florescent *E. coli* strain. The authors would also like to thank Dr. Boya Xiong for providing support needed to conduct streaming potential measurements. This work was supported by funding from the US National Science Foundation through the grants CBET-12022971, CBET–2027731, and CBET-1946392. Additional funding support was provided by the Department of Chemical Engineering at The Pennsylvania State University, a National Science Foundation REU program (EEC-1659497) and The Pennsylvania State University Global Programs, and the Welch Foundation (F-1696).

AUTHOR CONTRIBUTIONS

L.S., S.V., and M.K. conceived and designed the research. L.S., S.D., Y.-M.T., R.P.M., and M.G. performed the experiments with the assistance of H.O., C.H.A., A.R.-W., S.M., C.L., and J.M. L.S., S.V., and M.K. analyzed the data. R.C. performed the molecular docking simulations and wrote the relevant sections. L.S., S.V., and M.K. co-wrote the paper with editing help and comments from Y.-M.T., R.P.M., T.T., and D.G.

COMPETING INTERESTS

The authors declare no competing interests.

ADDITIONAL INFORMATION

Supplementary information The online version contains supplementary material available at https://doi.org/10.1038/s41545-022-00170-5.

Correspondence and requests for materials should be addressed to Manish Kumar.

Reprints and permission information is available at http://www.nature.com/reprints

Publisher's note Springer Nature remains neutral with regard to jurisdictional claims in published maps and institutional affiliations.